RSC Advances

PAPER

View Article Online
View Journal | View Issue

Check for updates

Cite this: *RSC Adv.*, 2020, **10**, 31874

Nano-Fe_3O_4@walnut shell/Cu(II) as a highly effective environmentally friendly catalyst for the one-pot *pseudo* three-component synthesis of 1,3-oxazine derivatives under solvent-free conditions†

Arefeh Dehghani Tafti and Bi Bi Fatemeh Mirjalili *

Received 13th May 2020
Accepted 8th August 2020

DOI: 10.1039/d0ra04282j

rsc.li/rsc-advances

Fe_3O_4@walnut shell/Cu(II) as an eco-friendly bio-based magnetic nano-catalyst was prepared by adding $CuCl_2$ to Fe_3O_4@walnut shell in alkaline medium. A series of 2-aryl/alkyl-2,3-dihydro-1*H*-naphtho[1,2-*e*][1,3]oxazines were synthesized by the one-pot *pseudo* three-component reaction of β-naphthol, formaldehyde and various amines using nano-Fe_3O_4@walnut shell/Cu(II) at 60 °C under solvent-free conditions. The catalyst was removed from the reaction mixture by an external magnet and was reusable several times without any considerable loss of its activity. This protocol has several advantages such as excellent yields, short reaction times, clean and convenient procedure, easy work-up and use of an eco-friendly catalyst.

Open Access Article. Published on 28 August 2020. Downloaded on 2/9/2026 9:10:56 PM.
This article is licensed under a Creative Commons Attribution-NonCommercial 3.0 Unported Licence.

Biopolymers, especially cellulose and its derivatives, have some unparalleled properties, which make them attractive alternatives for ordinary organic or inorganic supports for catalytic applications.[1] Cellulose is the most abundant natural material in the world and it can play an important role as a biocompatible, renewable resource and biodegradable polymer containing OH groups.[2] Walnut shell is a natural, cheap, and readily available source of cellulose. Fe_3O_4 nanoparticles are coated with various materials such as surfactants,[3] polymers,[4,5] silica,[6] cellulose[7] and carbon[8] to form core–shell structures. Magnetic nanoparticles as heterogeneous supports have many advantages such as high dispersion in reaction media and easy recovery by an external magnet.[9] Cu(II) as a safe and ecofriendly cation is a good Lewis acid and can activate the carbonyl group for nucleophilic addition reactions.[10]

1,3-Oxazines moiety has gained great attention from many organic and pharmaceutical chemists due to their broad range of biological activities such as anticancer,[11] anti-bacterial,[12] anti-tumor[13] and anti-Parkinson's disease.[14]

Owing to the biological importance of benzo-fused 1,3-oxazines, various methods have been developed for the synthesis of these compounds. Some shown protocols for the synthesis of various 2-aryl/alkyl-2,3-dihydro-1*H*-naphtho[1,2-*e*][1,3]oxazines *via* a Mannich type condensation between a 2-naphthol, formaldehyde and a primary amine were reported. This protocol has been catalyzed by $KAl(SO_4)_2 \cdot 12H_2O$ (alum),[15] $ZrOCl_2$,[16] polyethylene glycol (PEG),[17] thiamine hydrochloride (VB_1)[18] and CCl_3COOH.[19] Other methods of synthesis of oxazines are aza-acetalizations of aromatic aldehydes with 2-(*N*-substituted aminomethyl) phenols in the presence of an acid as catalyst[20] and electrooxidative cyclization of hydroxyamino compounds.[21]

However, some of these catalysts have limitations such as inefficient separation of the catalyst from reaction mixtures, unrecyclable and environmental limitations. Therefore, the development of green and clean methodology for the preparation of 2-aryl/alkyl-2,3-dihydro-1*H*-naphtho[1,2-*e*][1,3]oxazine derivatives is still an interesting challenge.

Herein, we wish to report the preparation of Fe_3O_4@nano-walnut shell/Cu(II) as a new and bio-based magnetic nanocatalyst and its using for one-pot synthesis of 1,3-oxazine derivatives *via* condensation of β-naphthol, primary amine and formaldehyde.

Results and discussion

The sequential step for the preparation of nano-Fe_3O_4@walnut shell/Cu(II) has been shown in Scheme 2. At first, nano-walnut shell was prepared from walnut shell using the previously reported method for preparation of nanocellulose.[7] Then, magnetic core–shell nanoparticles, nano-Fe_3O_4@walnut shell, were obtained simply through *in situ* co-precipitation of ferric and ferrous ions with ammonium hydroxide in an aqueous solution containing nano-walnut shell.[7] At the end, the nano-Fe_3O_4@walnut shell served as a magnetic support for the immobilization of Cu(II) by simple grinding with $CuCl_2 \cdot 2H_2O$ at room temperature (Scheme 1). The characterization of nano-Fe_3O_4@walnut shell/Cu(II), structure was performed by Fourier transform infrared (FT-IR) spectroscopy, X-ray diffraction (XRD), vibrating sample magnetometer (VSM), field emission

Department of Chemistry, College of Science, Yazd University, P.O. Box 89195-741, Yazd, Iran. E-mail: fmirjalili@yazd.ac.ir; Fax: +983538210644; Tel: +983531232672

† Electronic supplementary information (ESI) available. See DOI: 10.1039/d0ra04282j

This journal is © The Royal Society of Chemistry 2020

Open Access Article. Published on 28 August 2020. Downloaded on 2/9/2026 9:10:56 PM.
This article is licensed under a Creative Commons Attribution-NonCommercial 3.0 Unported Licence.

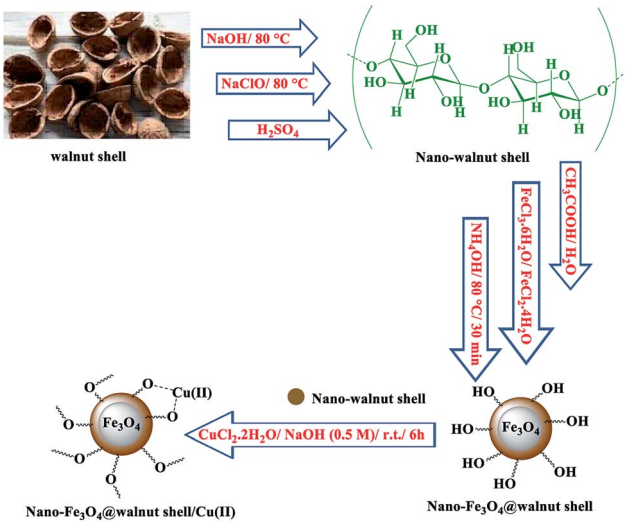

Scheme 1 Graphical representation preparation of nano-Fe_3O_4@walnut shell/Cu(II).

scanning electron microscopy (FESEM), energy-dispersive X-ray spectroscopy (EDS), and thermo-gravimetric analysis (TGA).

Fig. 1 shows the FT-IR spectra of nano-walnut shell, nano-Fe_3O_4@walnut shell and nano-Fe_3O_4@walnut shell/Cu(II). The FT-IR spectrum of nano-walnut shell (Fig. 1(a)), has shown a broad band at 3323 cm^{-1} which corresponds to the stretching vibrations of OH groups. The absorption bands at 1029–1160 cm^{-1} display the stretching vibrations of the C–O bonds.

For nano-Fe_3O_4@walnut shell (Fig. 1(b)), in addition to the walnut shell absorptions bands, stretching vibrations of Fe/O groups at 584 and 622 cm^{-1} are appeared which is indicated that the magnetic Fe_3O_4 nano particles are coated by nano-walnut shell. The FT-IR spectrum of nano-Fe_3O_4@walnut shell/Cu(II) (Fig. 1(c)) has shown a characteristic absorption band under 500 cm^{-1} that may be attributed to Cu–O band for Cu bonded to walnut shell.

The comparison between Fe_3O_4, nano-Fe_3O_4@walnut shell and nano-Fe_3O_4@walnut shell/Cu(II), XRD patterns in a range of 10–80° was shown in Fig. 2. In nano-Fe_3O_4@walnut shell XRD pattern, in addition to all peaks of naked Fe_3O_4 ($2\theta = 30°$, 35°, 43°, 53°, 57°, 63°, 71° and 73°), $2\theta = 23°$ confirmed the existence of walnut shell in its structure. The difference between XRD patterns of nano-

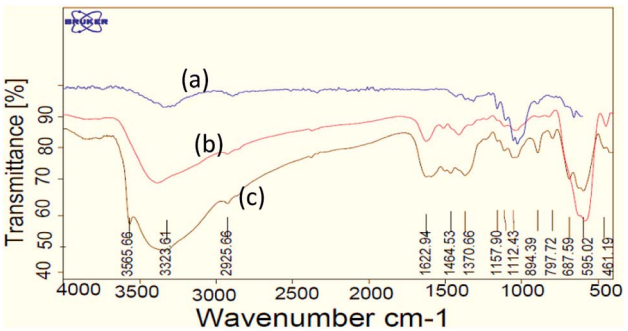

Fig. 1 FT-IR spectra of (a) nano-walnut shell, (b) nano-Fe_3O_4@walnut shell, (c) nano-Fe_3O_4@walnut shell/Cu(II).

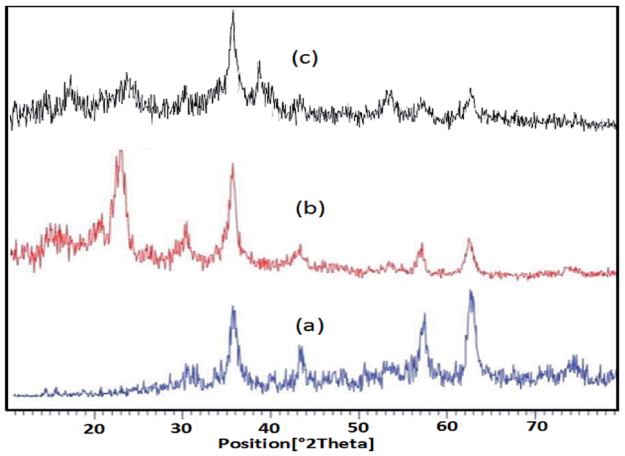

Fig. 2 XRD patterns of the (a) Fe_3O_4 (b) nano-Fe_3O_4@walnut shell, (c) nano-Fe_3O_4@walnut shell/Cu(II).

Fe_3O_4@walnut shell and nano-Fe_3O_4@walnut shell/Cu(II) shows the additional weak diffraction peaks at $2\theta = 39°$ and 54° in nano-Fe_3O_4@walnut shell/Cu(II), which seems to be linked to Cu(II) on the surface of nano-Fe_3O_4@walnut shell (Fig. 2(c)).

Fig. 3 represents the result of field emission scanning electron microscopy (FESEM) of nano-Fe_3O_4@walnut shell/Cu(II) to investigate its particle size and surface morphology. This image indicates that Fe_3O_4@walnut shell/Cu(II) nanoparticles have a quasi-spherical shape with an average size about 15 nm.

The magnetic properties of Fe_3O_4 and nano-Fe_3O_4@walnut shell/Cu(II) were characterized at RT (300 K) by a vibrating sample magnetometer (VSM) and their hysteresis curves are presented in Fig. 4. According to this image, the zero coercivity and remanence of the hysteresis loops of these magnetic nanoparticles confirm superparamagnetic property of them at room temperature. The amount of specific saturation magnetization (M_s) for Fe_3O_4 nanoparticles was about 47 emu g^{-1}, which decreased to 32 emu g^{-1} after coating the Fe_3O_4 with walnut shell and to 12 emu g^{-1} after the immobilization of Cu(II) on the surface of nano-Fe_3O_4@walnut shell. Despite this significant decrease, the saturated magnetization of these magnetic nanoparticles is sufficient for magnetic separation.

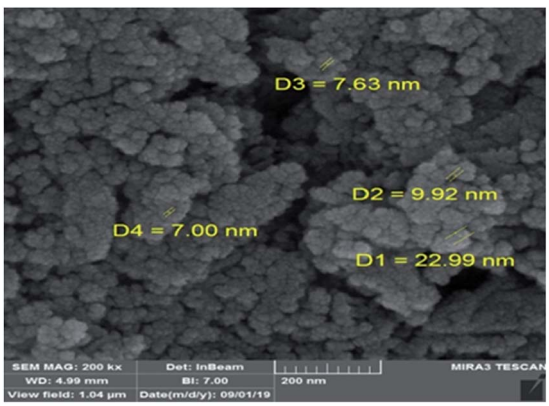

Fig. 3 FESEM image of nano-Fe_3O_4@walnut shell/Cu(II).

Open Access Article. Published on 28 August 2020. Downloaded on 2/9/2026 9:10:56 PM.
This article is licensed under a Creative Commons Attribution-NonCommercial 3.0 Unported Licence.

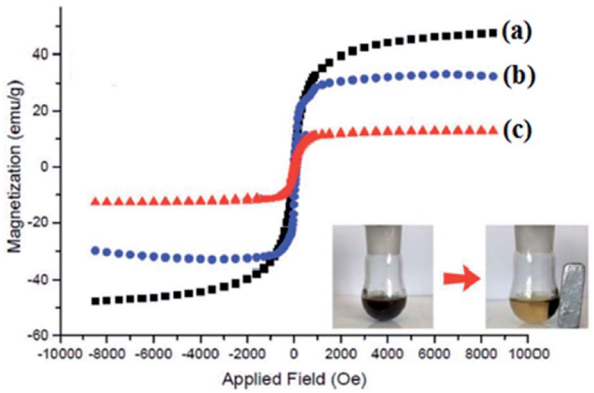

Fig. 4 Magnetization loops of (a) Fe_3O_4 (b) nano-Fe_3O_4@walnut shell, (c) nano-Fe_3O_4@walnut shell/Cu(II).

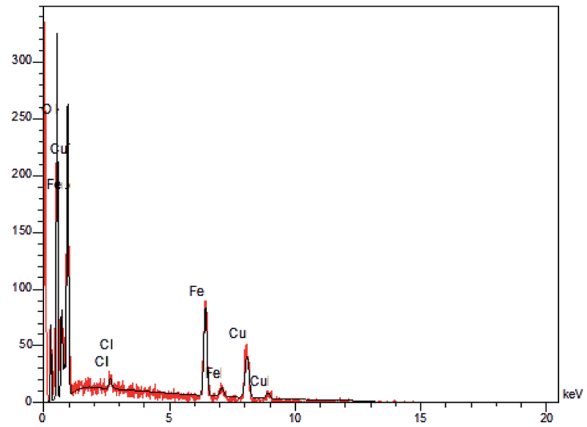

Fig. 6 EDX patterns of nano-Fe_3O_4@walnut shell/Cu(II).

TGA-DTA analysis was performed to study thermal stability of the nano-Fe_3O_4@walnut shell/Cu(II) in the temperature range of 50–810 °C (Fig. 5). The first decrease of weight was assigned to the catalyst moisture removal (endothermic effect at 50–190 °C, 8% weight loss). Subsequently, the main weight loss step in the temperature ranges 200–360 °C (34%) is attributed to the decomposition of walnut shell. The char yield of the catalyst in 810 °C is 42.16%.

The existence of the expected elements in the structure of the nano-Fe_3O_4@walnut shell/Cu(II) was approved by energy-dispersive X-ray spectroscopy EDS (EDX) analysis (Fig. 6). The EDS results clearly confirm the presence of Fe, O, Cu, C, Cl elements in the catalyst. The weight percentages of Fe, O, Cu, C and Cl are 19.48, 34.60, 26.09, 19.22 and 0.62%, respectively.

The catalytic activity of nano-Fe_3O_4@walnut shell/Cu(II) as a magnetically recyclable solid acid catalyst was investigated for the synthesis of 2-aryl/alkyl-2,3-dihydro-1*H*-naphtho[1,2-*e*][1,3]oxazine using three-component reaction of 2-naphthol, formaldehyde, and primary amines.

As a model reaction, the reaction between β-naphthol, formaldehyde, and aniline was investigated under various conditions (Table 1). As can be seen from Table 1, the highest yield was achieved by using 0.08 g catalyst at 60 °C under solvent-free condition (Table 1, entry 3). Other solvents such as H_2O, CH_2Cl_2, EtOH, CH_3CN, $CHCl_3$ and MeOH gave the desired products in low yields even after elongated reaction times in the same temperature (Table 1, entries 5–10).

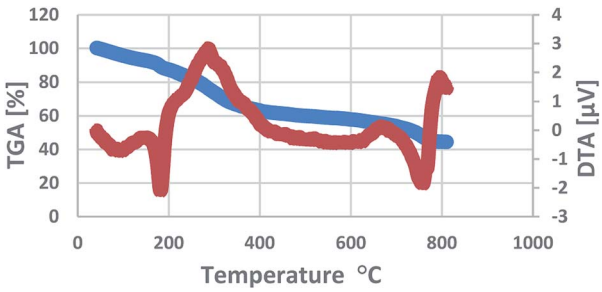

Fig. 5 Thermal gravimetric analysis pattern of nano-Fe_3O_4@walnut shell/Cu(II).

The model reaction was easier and gave the highest yield in solvent-free condition. Using the optimal reaction conditions, the scope and the versatility of this catalytic protocol were explored for the synthesis of various 2-aryl/alkyl-2,3-dihydro-1*H*-naphtho[1,2-*e*][1,3]oxazine (Table 2). The obtained results indicate that the reactions can proceed well enough with

Table 1 The reaction of β-naphthol, formaldehyde, and aniline in the presence of nano-Fe_3O_4@walnut shell/Cu(II) under various conditions[a]

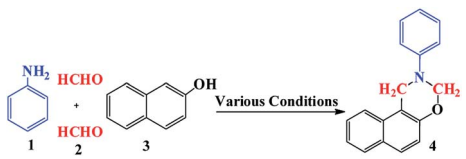

	Conditions		
Entry	Solvent/temp (°C)/catalyst (g)	Time (min)	Yield[b] (%)
1	—/r.t/catalyst (0.08)[c]	190	20
2	—/50/catalyst (0.08)[c]	45	88
3	—/60/catalyst (0.08)[c]	25	93
4	—/80/catalyst (0.08)[c]	50	75
5	H_2O/60/catalyst (0.08)[c]	45	73
6	CH_2Cl_2/60/catalyst (0.08)[c]	60	52
7	EtOH/60/catalyst (0.08)[c]	60	70
8	CH_3CN/60/catalyst (0.08)[c]	60	40
9	$CHCl_3$/60/catalyst (0.08)[c]	60	50
10	MeOH/60/catalyst (0.08)[c]	60	65
11	—/60/catalyst (0.04)[c]	50	85
12	—/60/catalyst (0.06)[c]	40	90
13	—/60/catalyst (0.07)[c]	25	90
14	—/60/catalyst (0.09)[c]	35	90
15	—/60/catalyst (0.1)[c]	60	60
16	—/60/—	200	5
17	—/60/nano-Fe_3O_4@walnut shell (0.08)	180	25
18	—/60/$CuCl_2$ (0.08)[c]	180	55

[a] The molar ratios are 1 : 2 : 3 is 1 : 2 : 1. [b] Isolated yield. [c] Nano-Fe_3O_4@walnut shell/Cu(II).

This journal is © The Royal Society of Chemistry 2020

Open Access Article. Published on 28 August 2020. Downloaded on 2/9/2026 9:10:56 PM.
This article is licensed under a Creative Commons Attribution-NonCommercial 3.0 Unported Licence.

Table 2 Synthesis of [1,3]oxazine derivatives in the presence of nano-Fe_3O_4@walnut shell/Cu(II) at 60 °C under solvent-free condition[a]

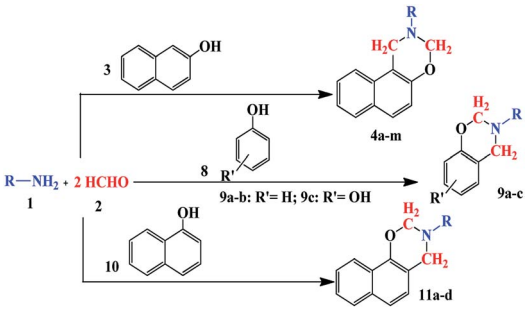

Entry	R	Product	Time (min)	Yield[b] (%)	Mp (°C) (ref.)
1	C_6H_5–	**4a**	25	93	45–47 (ref. 15)
2	4-Me–C_6H_4–	**4b**	15	92	87–89 (ref. 15)
3	4-Et–C_6H_4–	**4c**	25	90	44–46 (ref. 22)
4	4-Cl–C_6H_4–	**4d**	15	89	100–103 (ref. 18)
5	4-Br–C_6H_4–	**4e**	10	93	116–119 (ref. 15)
6	C_6H_5–CH_2–	**4f**	25	90	123–125 (ref. 23)
7	2-Cl–C_6H_4–CH_2–	**4g**	30	88	70–73 (ref. 22)
8	4-OMe–C_6H_4–	**4h**	15	85	75–77 (ref. 15)
9	C_6H_5–CH_2–CH_2–	**4i**	10	90	232(d) (ref. 22)
10	Cyclohexyl–	**4j**	15	90	248(d) (ref. 22)
11	*n*-Hexyl–	**4k**	25	89	177(d) (ref. 22)
12	2-Furyl–CH_2–	**4l**	30	92	98–100 (ref. 22)
13	*n*-Butyl–	**4m**	25	92	170(d) (ref. 22)
14	C_6H_5–	**9a**	40	85	59–62 (ref. 24)
15	4-Cl–C_6H_4–	**9b**	30	87	67–69 (ref. 25)
16	C_6H_5–	**9c**	25	88	75–76 (ref. 24)
17	C_6H_5–	**11a**	30	84	57–60 (ref. 16)
18	4-Cl–C_6H_4–	**11b**	25	87	107–109
19	4-OMe–C_6H_4–	**11c**	25	82	300(d) (ref. 16)
20	4-Me–C_6H_4–	**11d**	35	85	195–198 (ref. 16)

[a] The amount ratio of of primary amine (1 mmol), formaldehyde (2 mmol), β-naphthol, phenol or α-naphthol (1 mmol) equal to 1 : 2 : 1. [b] Isolated yield.

a relatively wide range of primary amines (aliphatic and aromatic) containing electron-donating and electron-withdrawing groups.

The structures of these products were characterized by physical and spectroscopic data such as mp, FT-IR, ^{1}H NMR, and ^{13}C NMR.

The separated nano-catalyst was reused in the mentioned reaction five times without considerable loss of its catalytic activity (Fig. 7). Meanwhile, FT-IR spectra of recovered catalyst were identical with the original catalyst spectra that indicating no considerable leaching of catalyst in reaction medium.

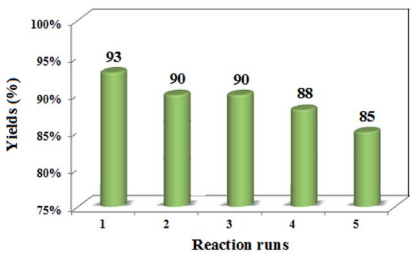

Fig. 7 Reusability of catalyst in the reaction between formaldehyde, aniline, and β-naphthol.

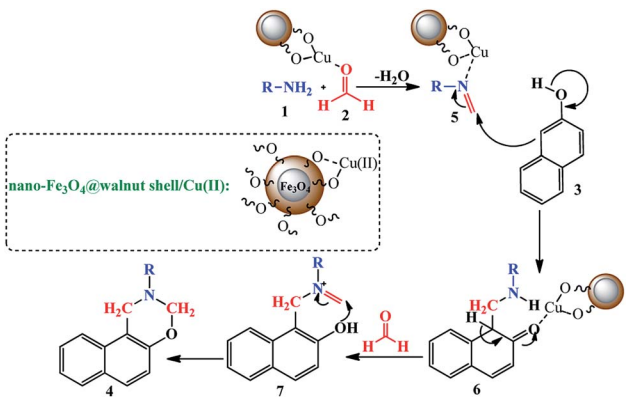

Scheme 2 Proposed mechanism for the synthesis of 1,3-oxazine derivatives.

Open Access Article. Published on 28 August 2020. Downloaded on 2/9/2026 9:10:56 PM.
This article is licensed under a Creative Commons Attribution-NonCommercial 3.0 Unported Licence.

Table 3 Catalytic performances of nano-Fe_3O_4@walnut shell/Cu(II) *versus* some other catalysts for synthesis of **4a**

	Conditions		
Entry	Solvent/temp (°C)/catalyst	Time (min)	Yield (%) (ref.)
1	—/60/[bmim]HSO_4	30	90 (ref. 26)
2	H_2O/r.t/thiamin hydrochloride (VB_1)	30	92 (ref. 18)
3	H_2O/r.t/—	30–60	79 (ref. 27)
4	H_2O/r.t/alum	10	85 (ref. 15)
5	H_2O/r.t/nano-Al_2O_3/BF_3/Fe_3O_4	20	90 (ref. 28)
6	Aqueous ethanol/r.t/Fe_3O_4@MAP	15	93 (ref. 29)
7	H_2O/r.t/$Fe(CF_3CO_2)_3$	25	86 (ref. 30)
8	—/60/catalyst[a]	25	93 (this work)

[a] Nano-Fe_3O_4@walnut shell/Cu(II).

A proposed mechanism for preparation of 2-aryl/alkyl-2,3-dihydro-1*H*-naphtho[1,2-*e*][1,3]oxazine in the presence of nano-Fe_3O_4@walnut shell/Cu(II) was shown in Scheme 2. Cu(II) activate the carbonyl group in formaldehyde and then Mannich-type condensation of the amine **1** and the formaldehyde **2** gives intermediate **5**. In the next step, the β-naphthol as a nucleophile attacked to the intermediate **5** to form intermediate **6** which was condense with the second molecule of formaldehyde to give intermediate **7**. Ultimately, by an intramolecular cyclization the 2-aryl/alkyl-2,3-dihydro-1*H*-naphtho[1,2-*e*][1,3]oxazine derivatives **4** were prepared.

As presented in Table 3, the use of nano-Fe_3O_4@walnut shell/Cu(II) resulted in an improved method in terms of reaction time, compatibility with environment, and yield when compared with other reported catalysts. From environmental friendly and simplicity of protocol viewpoints, the present report is one of the successful methods and is comparable with others. Meanwhile, magnetic property of the applied catalyst in this work cause simpler workup and recovery of catalyst than each other reported procedure.

Conclusions

In summary, we have demonstrated the preparation and characterization of nano-Fe_3O_4@walnut shell/Cu(II) as a novel magnetite recoverable, eco-friendly, inexpensive and efficient nanocatalyst. The catalytic activity of the prepared catalyst was investigated in the synthesis of 2-aryl/alkyl-2,3-dihydro-1*H*-naphtho[1,2-*e*][1,3]oxazine derivatives through one-pot three-component reaction of β-naphthol, formaldehyde, and primary amines under solvent-free condition at 60 °C. This protocol includes some important advantages such as mild reaction conditions, short reaction time, excellent yields, easy work-up, high purity of products. And so, magnetic separation and reusability of nanocatalyst is other advantages of this protocol.

Experimental

Materials and methods

Chemicals were purchased from Merck, Fluka, and Aldrich Chemical Companies. ^1H NMR and ^{13}C NMR spectra were recorded at 400 and 100 MHz, respectively. Fourier transform infrared (FT-IR) measurements (in KBr pellets or ATR) were recorded on a Brucker spectrometer. Melting points were determined on a Büchi B-540 apparatus. The X-ray diffraction (XRD) pattern was obtained by a Philips XpertMPD diffractometer equipped with a Cu Kα anode ($k = 1.54$ Å) in the 2θ range from 10 to 80°. Field Emission Scanning Electron Microscopy (FESEM) was obtained on a Mira 3-XMU. VSM measurements were performed by using a vibrating sample magnetometer (Meghnatis Daghigh Kavir Co. Kashan Kavir, Iran). Energy-dispersive X-ray spectroscopy (EDS) of nano-Fe_3O_4@ walnut shell/Cu(II) was measured by an EDS instrument and Phenom pro X. Thermal gravimetric analysis (TGA) was conducted using "STA 504" instrument.

Preparation of nano-walnut shell

Firstly, the walnut shell was heated in a boiling water for 15 minutes, dried and powdered. Then treated with a 17.5 w/v NaOH solution at 100 °C for 12 h under mechanical stirring. Subsequently, walnut shell was filtered and washed with distilled water until the alkali was completely eliminated. It was then bleached with 100 mL of 1 : 1 aqueous dilution of 3.5% w/v sodium hypochlorite at 80 °C for 3 h under mechanical stirring. The resulting alpha cellulose was hydrolyzed partially using 65% sulfuric acid aqueous solution with a walnut shell-to-acid weight ratio of 1–10 at 45 °C. After 1 h, the obtained suspension was diluted with water five-fold to stop the hydrolysis reaction. The suspension was centrifuged at 4000 rpm to separate the nano-walnut shell from acid solution. The washing with water and centrifuging was repeated four to five times to remove any remaining free acid. The yield of obtained nano-walnut shell is 60%.

Preparation of nano-Fe_3O_4@walnut shell

1 g of nano-walnut shell was dissolved in 100 mL of 0.05 M acetic acid solution; to which $FeCl_3 \cdot 6H_2O$ (3.51 g, 0.013 mol) and $FeCl_2 \cdot 4H_2O$ (1.29 g, 0.0065 mol) were added. The mixture was stirred for 4 h at 80 °C. As a result, 6 mL of 25% NH_4OH was added drop wise into the reaction mixture with constant stirring. After 30 min, the mixture was cooled to room temperature

 This journal is © The Royal Society of Chemistry 2020

Open Access Article. Published on 28 August 2020. Downloaded on 2/9/2026 9:10:56 PM.
This article is licensed under a Creative Commons Attribution-NonCommercial 3.0 Unported Licence.

and then by using an external magnet, nano walnut shell coated over magnetic nanoparticles were separated. Then magnetic precipitate first was washed with distilled water then ethanol, and finally dried at 80 °C for 4 h. The final weight of obtained nano-Fe_3O_4@walnut shell is 1.5 g.

Preparation of nano-Fe_3O_4@walnut shell/Cu(II)

In a flask containing 50 mL of 0.5 M NaOH, nano-Fe_3O_4@walnut shell (0.5 g) was added with stirring. Then, 75 mL of $CuCl_2$ aqueous solution, 0.04 M, was added. A dark brown solution was obtained immediately that was stirred at room temperature. After 6 h, the magnetically heterogeneous catalyst, nano-Fe_3O_4@walnut shell/Cu(II), removed from solution by an external magnet. The catalyst washed with ethanol and water two times and dried at an oven at 80 °C.

General procedure for synthesis of 2-aryl/alkyl-2,3-dihydro-1*H*-naphtho[1,2-*e*][1,3]oxazine

A mixture of β-naphthol (1.0 mmol), primary amine (1.0 mmol) and formaldehyde 37% (2.0 mmol/0.07 mL) and nano-Fe_3O_4@walnut shell/Cu(II) (0.08 g) was stirred at 60 °C under solvent-free condition. After completion of the reaction that monitored by TLC, the reaction mixture was dissolved in hot ethanol (3 mL) and the catalyst was separated by using an external magnet. Then, cold water was added to residue and the solid product was collected by filtration. Almost in all cases, the products were pure and showed the expected analytical data. The recovered catalyst was washed several times with ethanol, dried, and reused for next runs.

Spectral data for selected compounds

2-(4-Chlorophenyl)-2,3-dihydro-1*H*-naphtho[1,2-*e*][1,3]oxazine (Table 2, 4d). White solid, mp 100–103 °C. FT-IR (ATR) $\bar{\nu}$ (cm^{-1}): 1593, 1492, 1225, 1092. ^{1}H NMR (acetone-d_6, 400 MHz)/δ ppm: 7.84 (t, 2H, ^3J = 9.2 Hz, Ar–H), 7.71 (d, 1H, ^3J = 8.8 Hz, Ar–H), 7.53 (t, 1H, ^3J = 7.2 Hz, Ar–H), 7.38 (t, 1H, ^3J = 7.6 Hz, Ar–H), 7.24–7.29 (m, 4H, Ar–H), 7.02 (d, 1H, ^3J = 8.8 Hz, Ar–H), 5.51 (s, 2H, O–CH_2–N), 5.03 (s, 2H, –Ar–CH_2–N).

2-Cyclohexyl-2,3-dihydro-1*H*-naphtho[1,2-*e*][1,3]oxazine (Table 2, 4j). Off-white solid, mp 248 °C (d). FT-IR (ATR) $\bar{\nu}$ (cm^{-1}): 2926, 2852, 1597, 1467, 1227, 1058. ^{1}H NMR (DMSO-d_6, 500 MHz)/δ ppm: 7.66–7.81 (m, 3H, Ar–H), 7.48 (m, 1H, Ar–H), 7.35 (m, 1H, Ar–H), 6.98 (m, 1H, Ar–H), 4.99 (s, 2H, O–CH_2–N), 4.33 (s, 2H, Ar–CH_2–N), 2.70 (m, 1H, CH–N), 1.08–1.86 (m, 10H, 5CH_2).

2-Hexyl-2,3-dihydro-1*H*-naphtho[1,2-*e*][1,3]oxazine (Table 2, 4k). Brown solid, mp 177 °C (d). FT-IR (ATR) $\bar{\nu}$ (cm^{-1}): 2927, 2854, 1597, 1467, 1225, 1057. ^{1}H NMR (DMSO-d_6, 500 MHz)/δ ppm: 7.80 (m, 1H, Ar–H), 7.68 (m, 2H, Ar–H), 7.47 (m, 1H, Ar–H), 7.34 (m, 1H, Ar–H), 7.00 (m, 1H, Ar–H), 4.87 (s, 2H, O–CH_2–N), 4.25 (s, 2H, –Ar–CH_2–N), 2.68 (m, 2H, –CH_2–N), 1.53 (m, 2H, CH_2), 1.25 (m, 6H, 3CH_2), 0.84 (m, 3H, CH_3). ^{13}C NMR (DMSO-d_6, 125 MHz)/δ ppm: 14.77, 22.98, 27.23, 28.38, 32.02, 47.87, 52.09, 82.71, 112.97, 119.14, 122.18, 124.13, 127.32, 128.46, 129.21, 129.28, 132.44, 152.42.

Conflicts of interest

There are no conflicts to declare.

Acknowledgements

The Research Council of Yazd University gratefully acknowledged for the financial support for this work.

Notes and references

1 (*a*) D. Klemm, B. Heublein, H. P. Fink and A. Bohn, *Angew. Chem., Int. Ed.*, 2005, **44**, 3358–3393; (*b*) Y. Habibi, L. A. Lucia and O. J. Rojas, *Chem. Rev.*, 2010, **110**, 3479–3500; (*c*) R. J. Moon, A. Martini, J. Nairn, J. Simonsen and J. Youngblood, *Chem. Soc. Rev.*, 2011, **40**, 3941–3994; (*d*) S. Van de Vyver, J. Geboers, P. A. Jacobs and B. F. Sels, *ChemCatChem*, 2011, **3**, 82–94; (*e*) F. Rol, M. N. Belgacem, A. Gandini and J. Bras, *Prog. Polym. Sci.*, 2019, **88**, 241–264.

2 (*a*) A. Shaabani and A. Maleki, *Appl. Catal., A*, 2007, **331**, 149–151; (*b*) H. P. S. Khalil, Y. Y. Tye, C. K. Saurabh, C. P. Leh, T. K. Lai, E. W. N. Chong, M. R. Fazita, J. Mohd Hafiidz, A. Banerjee and M. I. Syakir, *eXPRESS Polym. Lett.*, 2017, **11**, 244–265; (*c*) V. P. Cyras, C. M. Soledad and V. Analía, *Polym*, 2009, **50**, 6274–6280; (*d*) J. Credou and T. Berthelot, *J. Mater. Chem. B*, 2014, **2**, 4767–4788; (*e*) G. Cipriani, A. Salvini, P. Baglioni and E. Bucciarelli, *J. Appl. Polym. Sci.*, 2010, **118**, 2939–2950; (*f*) I. Siró and D. Plackett, *Cellulose*, 2010, **17**, 459–494.

3 Y. Lu, X. Lu, B. T. Mayers, T. Herricks and Y. Xia, *J. Solid State Chem.*, 2008, **181**, 1530–1538.

4 H. F. Rase, *Handbook of Commercial Catalysts: Heterogeneous Catalysts*, CRC Press, New York, 2000.

5 A. El Harrak, G. Carrot, J. Oberdisse, C. Eychenne-Baron and F. Boué, *Macromolecules*, 2004, **37**, 6376–6384.

6 P. Tartaj and C. J. Serna, *J. Am. Chem. Soc.*, 2003, **125**, 15754–15755.

7 S. Azad and B. F. Mirjalili, *RSC Adv.*, 2016, **6**, 96928–96934.

8 Z. Zhang, H. Duan, S. Li and Y. Lin, *Langmuir*, 2010, **26**, 6676–6680.

9 M. A. Zolfigol, A. R. Moosavi-Zare, P. Moosavi, V. Khakyzadeh and A. Zare, *C. R. Chim.*, 2013, **16**, 962–966.

10 N. Safajoo, B. F. Mirjalili and A. Bamoniri, *RSC Adv.*, 2019, **9**, 1278–1283.

11 K. S. Kumar, N. P. Kumar, B. Rajesham, G. Kishan, S. Akula and R. K. Kancha, *New J. Chem.*, 2018, **42**, 34–38.

12 N. Latif, N. Mishriky and F. Massad, *Aust. J. Chem.*, 1982, **35**, 1037–1043.

13 J. B. Chylinska and T. Urbanski, *J. Med. Chem.*, 1963, **6**, 484–487.

14 W. J. Weiner, S. A. Factor and J. R. Sanchez-Ramos, *J. Neurol., Neurosurg. Psychiatry*, 1989, **52**, 732–735.

15 S. A. Sadaphal, S. S. Sonar, B. B. Shingate and M. S. Shingare, *Green Chem. Lett. Rev.*, 2010, **3**, 213–216.

16 A. H. Kategaonkar, S. S. Sonar, R. U. Pokalwar, A. H. Kategaonkar, B. B. Shingate and M. S. Shingare, *Bull. Korean Chem. Soc.*, 2010, **31**, 1657–1660.

Open Access Article. Published on 28 August 2020. Downloaded on 2/9/2026 9:10:56 PM.
This article is licensed under a Creative Commons Attribution-NonCommercial 3.0 Unported Licence.

17 P. V. Shinde, A. H. Kategaonkar, B. B. Shingate and M. S. Shingare, *Chin. Chem. Lett.*, 2011, **22**, 915–918.
18 V. D. Dhakane, S. S. Gholap, U. P. Deshmukh, H. V. Chavan and B. P. Bandgar, *C. R. Chim.*, 2014, **17**, 431–436.
19 R. Borah, A. K. Dutta, P. Sarma, C. Dutta and B. Sarma, *RSC Adv.*, 2014, **4**, 10912–10917.
20 Z. Tang, Z. Zhu, Z. Xia, H. Liu, J. Chen, W. Xiao and X. Ou, *Molecules*, 2012, **17**, 8174–8185.
21 M. Okimoto, K. Ohashi, H. Yamamori, S. Nishikawa, M. Hoshi and T. Yoshida, *Synthesis*, 2012, **44**, 1315–1322.
22 S. Azad and B. F. Mirjalili, *Mol. Diversity*, 2019, **23**, 413–420.
23 S. S. Ganesan, N. Rajendran, S. I. Sundarakumar, A. Ganesan and B. Pemiah, *Synthesis*, 2013, **45**, 1564–1568.
24 R. Andreu and J. C. Ronda, *Synth. Commun.*, 2008, **38**, 2316–2329.
25 Z. Tang, W. Chen, Z. Zhu and H. Liu, *Synth. Commun.*, 2012, **42**, 1372–1383.
26 S. B. Sapkal, K. F. Shelke, B. B. Shingate and M. S. Shingare, *J. Korean Chem. Soc.*, 2010, **54**, 437–442.
27 B. P. Mathew and M. Nath, *J. Heterocycl. Chem.*, 2009, **46**, 1003–1006.
28 E. Babaei and B. F. Mirjalili, *Polycyclic Aromat. Compd.*, 2019, 1–8.
29 R. Nongrum, M. Kharkongor, G. S. Nongthombam, N. Rahman, G. K. Kharmawlong and R. Nongkhlaw, *Environ. Chem. Lett.*, 2019, **17**, 1325–1331.
30 T. Lohar, A. Mane, S. Kamat and R. Salunkhe, *Polycyclic Aromat. Compd.*, 2018, 1–13.

This journal is © The Royal Society of Chemistry 2020